Enhancing the Current Density of Electrodeposited ZnO-Cu_2O Solar Cells by Engineering their Heterointerfaces

Ahmad Sabirin Zoolfakar[a,d,*] Rozina Abdul Rani[a], Anthony J. Morfa[b], Sivacarendran Balendhran[a], Anthony P. O'Mullane[c], Serge Zhuiykov[e] and Kourosh Kalantar-zadeh[a,*]

[a] School of Electrical and Computer Engineering, RMIT University, Melbourne VIC 3001 Australia

[b]School of Chemistry & Bio21 Institute, University of Melbourne, ParkVille, Victoria, 3010, Australia

[c]School of Applied Sciences, RMIT University, Melbourne VIC 3001 Australia

[d] Faculty of Electrical Engineering, Universiti Teknologi MARA, 40450 Shah Alam Malaysia

[e] Materials Science and Engineering Division, CSIRO, Highett, VIC, Australia

E-mail: a.zoolfakar@student.rmit.edu.au and kourosh.kalantar@rmit.edu.au

X-ray photoelectron spectroscopy (XPS) analysis of electrodeposited ZnO thin films grown onto rf sputtered powers ZnO seed layers at different powers

Fig. S1 shows XPS spectra of electrodeposited ZnO thin films grown onto rf sputtered powers ZnO seed layers at different powers. All the films exhibited high peak intensity correspond to (a) zinc and (b) oxygen.

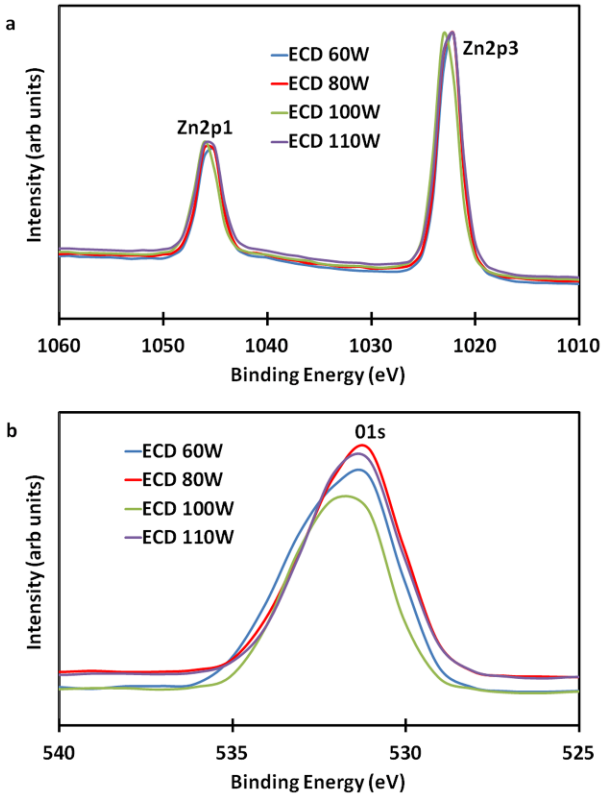

Fig. S1 XPS spectra of electrodeposited ZnO thin films grown onto rf sputtered powers ZnO seed layers at different powers. All the films exhibited high peak intensity correspond to (a) zinc and (b) oxygen

Raman Spectra analysis of electrodeposited ZnO thin films grown onto rf sputtered powers ZnO seed layers at different powers

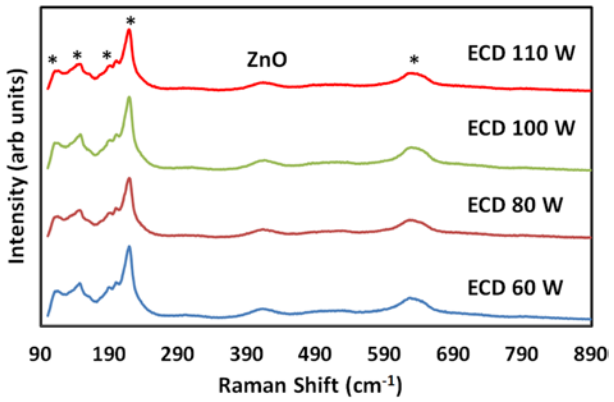

Fig. S2 Raman spectra of ZnO-Cu_2O films: as described in Fig. 7. The ZnO electrodeposited films are formed onto rf sputtered ZnO seed layers, which are deposited onto FTO substrate

For a more precise determination of phase composition of the films, Raman spectra were also obtained and presented in Fig. S2. The Cu_2O peaks were noted with asterisks. Three peaks located at 110, 146 and 217 cm^{-1} are observed and ascribed to Cu_2O.[8-10] The broad peaks centred at 512 and 626 cm^{-1} are also believed to be contributed by Cu_2O.[9] A ZnO peak is also observed at 407 cm^{-1} associated with the E_2 vibration of the wurtzite lattice.[11, 12] The Raman spectra of ZnO-Cu_2O films agree well with the XRD results for sample composition identification.

Plot of force as a function of time

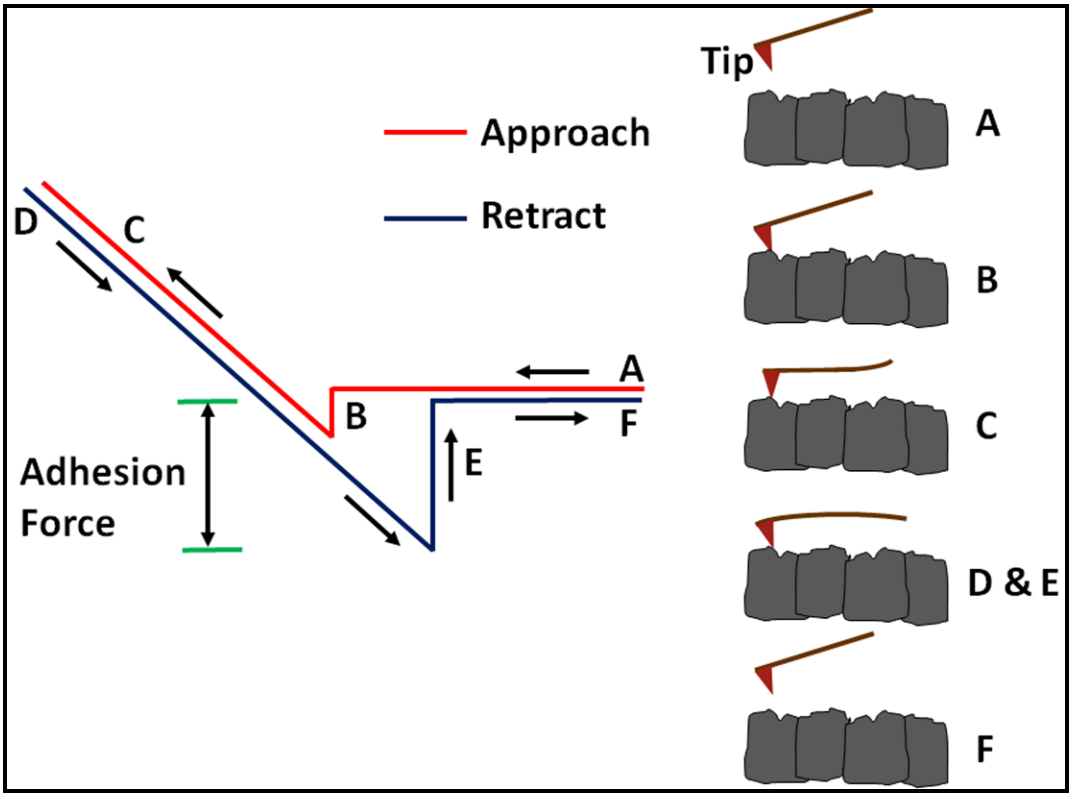

Fig. S3 A typical force-curve describing a single approach-retract cycle of the AFM tip. (A) The AFM tip is approaching the sample surface. (B) The initial contact between the tip and the surface is mediated by the attractive van der Waals forces (contact) that lead to an attraction of the tip toward the surface. (C) The tip applies a constant and default force upon the surface that leads to sample indentation and cantilever deflection. (D) Subsequently, the tip tries to retract and to break loose from the surface. (E) Various adhesive forces between the sample and the AFM tip, however, hinder tip retraction. These adhesive forces can be taken directly from the force-distance curve. (F) The tip withdraws and loose contact to the surface upon overcoming the adhesive forces.[7]

Direct observation - SEM cross section image of electrodeposited ZnO-Cu_2O heterojunction

We also carried out direct observation of cross section images of heterointerface electrodeposited ZnO-Cu_2O grown onto different rf sputtered ZnO seed layers (a) 60 W, (b) 80 W, (c) 100 W and (d) 110 W using FEI Nova NanoSEM. Based on the SEM images, we observe that the heterointerface for the 60W sample is the most different from the other three. It seems that the Cu_2O interface for the 60W sample is made of less crystalline materials, and does not have the perfect crystal grain perfection that are specifically seen in the 80 and 100 W samples after cleaving the films.

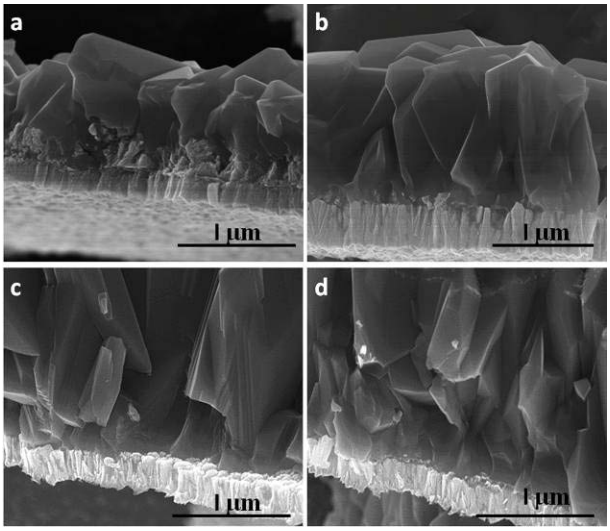

Fig. S4 SEM cross section image of electrodeposited ZnO-Cu_2O heterojunction grown onto different rf sputtered ZnO seed layers (a) 60 W, (b) 80 W, (c) 100 W and (d) 110 W

Study the effect of ZnO and Cu_2O film thickness on solar cells performance

The experiments were conducted in two phases. The first phase was to study the effect of ZnO film thickness on PCE, as the thicknesses of heterojunction films greatly affects the efficiency of solar cells.[1-3] Increasing the film thickness generally increases the internal resistance of the device, which reduces the fill factor and, consequently, efficiency.[3] Additionally, the built-in electric field also changes with the thickness of the films.[1] In this experiment, we fixed the zinc nitrate concentration to 0.05 M, the temperature was fixed at 62 ºC and electrodeposition was carried out potentiostatically at –0.7 V without stirring. We used a rf sputtered ZnO seed layer at 100 W onto FTO substrates and then varied the electrodeposition time of the second ZnO layer from 300 to 2000 s in order to obtain different thicknesses. Then the Cu_2O layer was electrodeposited for 2000 s at –0.55 V, pH 13.5, T_{sol} = 40 ºC to give a thickness of approximately 1.8 μm. Finally, a circular Au contact pad was sputtered on the top of the Cu_2O film to act as a contact electrode for photovoltaic testing. Table S1 summarizes the photovoltaic properties of the devices. From Table S1, an electrodeposition time of 1000 s produces the largest $J_{sc,}$ V_{oc}, FF and PCE values of 10.8 mA/cm^2, 0.29 V, 31.4% and 0.95%, respectively. The combination of a ZnO seed layer and electrodeposition for the duration of 1000 s produced a 450 nm thick ZnO film.

The second phase of the experiments was to study the effect of Cu_2O electrodeposition duration in order to determine an optimum thickness for the Cu_2O films. In this experiment, we used the same conditions as in Table S1 for the ZnO electrodeposited films of 1000 s duration. We fabricated five samples with Cu_2O electrodeposition durations ranging from 1000 to 2500 s. The Cu_2O layer was electrodeposited at –0.55 V, pH of 13.5 and T_{sol} = 40 ºC. The electrodeposition duration of 2000 s (1.8 μm thickness) produced the highest FF and PCE of 31.4 % and 0.95 %, respectively. This is in agreement with the work of other researchers who demonstrated that the Cu_2O thickness should be larger than the ZnO thickness, as the free carrier concentration of Cu_2O is much smaller than ZnO.[4-6] Full photovoltaic properties are listed in Table S2.

SUPPORTING INFORMATION

Table S1. Photovoltaic properties of ZnO-Cu_2O solar cells with different ZnO electrodeposition durations

ZnO electrodeposition durations (s)	J_{SC} (mA/cm^2)	V_{OC} (V)	FF (%)	PCE (%)
300	9.11	0.21	27.8	0.51
600	5.81	0.24	15.8	0.22
1000	10.8	0.29	31.4	0.95
1500	10.3	0.25	25.7	0.65
2000	0.49	0.16	29.6	0.02

ZnO electrodeposition was performed onto rf sputtered ZnO with power of 100 W. The Cu_2O layer was electrodeposited at −0.55 V, pH of 13.5, T_{sol} = 40 ºC and duration of 2000 s.

Table S2. Photovoltaic properties of ZnO-Cu_2O solar cells with different Cu_2O electrodeposition durations

Cu_2O electrodeposition durations (s)	J_{SC} (mA/cm^2)	V_{OC} (V)	FF (%)	PCE (%)
1000	1.05	0.155	16.9	0.03
1500	4.99	0.168	24.6	0.21
1800	11.1	0.262	28.9	0.84
2000	10.8	0.285	31.4	0.95
2500	6.34	0.197	28.9	0.36

Cu_2O electrodeposition was performed onto combination of electrodeposition ZnO and rf sputtered ZnO with power of 100 W.

Reproducibility of solar cell performance

In order to verify the reproducibility of the solar cells performance, we fabricated 6 different samples for each type of ZnO-Cu_2O heterojunction solar cells (i.e. FTO, 60 W, 80 W, 100 W and 110 W). Figure S5 shows the average of short circuit current density and open circuit voltage photo-response of the ZnO-Cu_2O heterojunction based solar cells. The tests were performed six times.

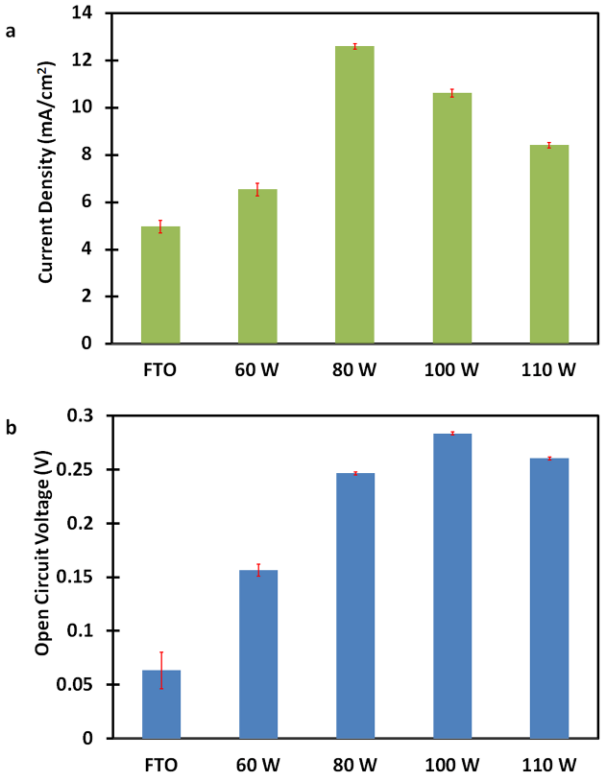

Fig. S5 Average of short circuit current density and open circuit voltage values for five types of ZnO-Cu_2O heterojunction solar cells. The tests were performed on six similarly fabricated samples.

References

1. D. W. Sievers, V. Shrotriya and Y. Yang, *J. Appl. Phys.*, 2006, **100**, 114509.
2. J. Peet, J. Y. Kim, N. E. Coates, W. L. Ma, D. Moses, A. J. Heeger and G. C. Bazan, *Nat. Mater.*, 2007, **6**, 497–500.
3. S. H. Park, A. Roy, S. Beaupre, S. Cho, N. Coates, J. S. Moon, D. Moses, M. Leclerc, K. Lee and A. J. Heeger, *Nat. Photonics*, 2009, **3**, 297–302.
4. H. Wei, H. Gong, Y. Wang, X. Hu, L. Chen, H. Xu, P. Liu and B. Cao, *Crystengcomm*, 2011, **13**, 6065–6070.
5. K. P. Musselman, A. Marin, A. Wisnet, C. Scheu, J. L. MacManus-Driscoll and L. Schmidt-Mende, *Adv. Funct. Mater.*, 2011, **21**, 573–582.
6. J. B. Cui and U. J. Gibson, *J. Phys. Chem. B*, 2010, **114**, 6408–6412.
7. V. Shahin, Y. Ludwig, C. Schafer, D. Nikova and H. Oberleithner, *Journal of Cell Science*, 2005, **118**, 2881–2889.
8. A. Compaan and H. Z. Cummins, *Phys. Rev. B*, 1972, **6**, 4753–4757.
9. Y. M. Lu, J. Y. Chen and T. S. Wey, *Mater. Res. Soc. Symp. P*, 2004, **822**, 55–64.
10. L. Wu, L.-k. Tsui, N. Swami and G. Zangari, *J. Phys. Chem. C*, 2010, **114**, 11551–11556.
11. K. A. Alim, V. A. Fonoberov, M. Shamsa and A. A. Balandin, *J. Appl. Phys.*, 2005, **97**, 124313.
12. A. Chatterjee and J. Foord, *Diam. Relat. Mater.*, 2006, **15**, 664–667.